Article

JOURNAL OF COMPOSITE MATERIALS

Journal of Composite Materials
2017, Vol. 51(3) 333–355

DOI: 10.1177/0021998316645171
journals.sagepub.com/home/jcm
SAGE

Effect of high temperature on structural response of reinforced concrete circular columns strengthened with fiber reinforced polymer composites

Hussein Elsanadedy, Tarek Almusallam, Yousef Al-Salloum and Rizwan Iqbal

Abstract

This research investigates the effect of elevated temperature on behavior of reinforced concrete (RC) circular columns strengthened with different fiber reinforced polymer (FRP) systems. For this purpose, 32 column specimens were prepared. The test matrix comprised: 14 unstrengthened columns, 14 columns strengthened with a single layer of CFRP sheet, and 4 specimens strengthened with a single layer of GFRP sheet. Out of the 14 CFRP-wrapped specimens, 4 columns were thermally insulated with commercially available fire-protection mortar. In addition to control specimens at room temperature, some other columns were subjected to high temperature regimes of 100°C, 200°C, 300°C, 400°C, 500°C, and 800°C for a period of 3 h. After cooling down, the columns were tested under axial compression until failure. It was indicated that exposure to elevated temperature adversely affected the residual strength, stiffness, and axial/lateral stress–strain response of unstrengthened columns. FRP composites were found effective in enhancing the axial load capacity of exposed columns provided that the temperature at the FRP level does not exceed the decomposition limit of the epoxy resin. The degradation in strength and stiffness was higher in CFRP-strengthened columns compared with GFRP-strengthened columns when exposed to the same temperature level. The used insulation material was found efficient in preventing heat induced damage to CFRP-strengthened columns up to temperature of 800°C for 3 h duration. Besides this study, the experimental data of 48 uninsulated FRP-strengthened circular concrete specimens subjected to different heating regimes were collected from the literature. The dataset of 55 uninsulated FRP-strengthened specimens was then employed to evaluate the ACI 440.2R-08 model used for assessing compressive strength of FRP-confined concrete. This model was found non-conservative for 48.6% of the data and thus it was revised by the inclusion of an FRP strength reduction factor due to heating, which can be utilized in the design of FRP-strengthened RC columns exposed to elevated temperature.

Keywords

Fiber reinforced polymers, RC columns, high temperature, strengthening, ultimate strength

Introduction

Strengthening of reinforced concrete (RC) columns is required for several reasons such as extension of their lifetime, column degradation due to lack of maintenance, and the need to carry more loads than their designed values. Several strengthening measures have been developed by researchers and practicing engineers for RC columns. One of the most recently used techniques involves wrapping of RC columns by fiber reinforced polymer (FRP) composites to provide confinement for strength and ductility enhancement. FRP composites present an attractive option due to several reasons such as their high strength-to-weight

Department of Civil Engineering, King Saud University, Saudi Arabia

Corresponding author:
Hussein Elsanadedy, MMB Chair for Research and Studies in Strengthening and Rehabilitation of Structures, Department of Civil Engineering, College of Engineering, King Saud University, P.O. Box 800, Riyadh 11421, Saudi Arabia.
Email: helsanadedy@ksu.edu.sa

and stiffness-to-weight ratios, large deformation capacity, minimal change in the geometry, corrosion resistance to environmental degradation, and speed of application. Use of FRP jackets to strengthen RC columns has been studied by several investigators.[1–14]

The application of externally bonded FRP composites in structures, yet, has been mired due to uncertainties concerning their performance in fire or elevated temperature environments. FRP composites are vulnerable to ignition of their polymer matrix. Furthermore, strength and stiffness of polymer matrices get significantly reduced if heated above their glass transition temperature (T_g). Hence, if left uninsulated, FRP composites may ignite with increased flame spread and toxic smoke evolution, and they may quickly lose bond and/or mechanical properties.[15,16] Therefore, the behavior of FRP-strengthened RC columns exposed to fire or elevated temperature environments is of big concern. As yet, research in this area is limited, and more work is needed. The objective of current study is to fill some of the gaps in learning the behavior of RC structures strengthened with FRPs and exposed to high temperature.

Related work

Research in this area is categorized into two branches *viz*. one related to performance of FRP-wrapped concrete columns after being exposed to elevated temperature regimes to assess their residual capacity,[17–21] and the second pertains to behavior of preloaded FRP-strengthened columns under standard fire tests.[22,23] For both branches, limited research exists in the literature.

In a study by Cleary et al.,[17] GFRP-wrapped concrete cylinders were subjected to high temperatures ranging from 120°C to 180°C, left to cool down to ambient temperature and then loaded in axial compression till failure. There was no significant reduction of compressive strength until the elevated temperature was more than 30°C above T_g of the epoxy. The study also concluded that the application of fire protection material minimized the loss of compressive strength in columns exposed to high temperatures. The effect of high temperature on GFRP-wrapped concrete cylinders was studied experimentally by Saafi and Romine.[18] The GFRP composite laminates had a severe damage due to creep and melting of epoxy when the specimens were heated at a temperature equal to or above T_g of the epoxy matrix. Al-Salloum et al.[19] studied experimentally the effect of elevated temperature on the behavior of CFRP- and GFRP-wrapped concrete cylinders after being exposed to high temperatures of 100°C and 200°C for a period of 1, 2, or 3 h. At a temperature of 100°C (slightly higher than T_g of the epoxy), wrapped cylinders had small reductions in strength. The loss of strength was more evident for a temperature of 200°C. Khalifa et al.[20] assessed experimentally the residual capacity of thermally insulated CFRP-strengthened RC square columns after being heated to temperatures ranging from 70°C to 350°C, for different durations of 4, 8, 12, and 24 h. The use of insulation material enhanced the thermal endurance of the columns to a certain extent. Reduction of axial strength of columns was insignificant for temperature up to 100°C for 24 h duration. Yet, for temperatures above 100°C, the residual column capacity depended mostly on the exposure duration. El-Karmoty[21] studied experimentally the behavior of GFRP-wrapped RC circular columns thermally insulated with two types of fire protection systems after being exposed to 600°C for a duration of 1 and 2 h, respectively. The use of insulation materials increased the ultimate load of the columns (with respect to the uninsulated column), but the ultimate loads of the insulated columns were still smaller than that of the unheated GFRP-wrapped column.

For behavior in fire of FRP-wrapped RC columns, Chowdhury et al.[22] conducted standard fire tests on two FRP-strengthened columns (with and without supplemental fire protection system). The insulated column was able to resist elevated temperatures during the fire test for at least 90 min longer than the equivalent uninsulated column. However, even though the second column was thermally insulated, the temperature at the FRP/concrete interface surpassed T_g of the epoxy at about 34 min into the fire test. This indicates that the used insulation system was probably not able to safeguard the FRP system, which is widely thought to degrade at temperatures beyond its T_g. However, even though the FRP-strengthening system was presumed to have been rendered ineffective by the end of the fire tests, the loss of strength of the two columns was significantly different. The uninsulated column failed under the sustained load after 210 min of exposure and its tested strength was lower than the factored design strength of an equivalent unwrapped column. Yet, the insulated column failed after 5 h of fire exposure at a load 59% higher than the factored strength of an equivalent unwrapped column. In another study, Cree et al.[23] investigated experimentally the behavior in fire of two insulated CFRP-strengthened RC columns (one circular and one square). The columns were subjected to the CAN/ULC S101[24] standard fire tests. The insulation system was efficient in protecting the columns such that they were able to reach 4 h fire endurance ratings in accordance with CAN/ULC S101[24] and ASTM E119.[25] Yet, the fire protection material couldn't keep the temperature of the FRP below its T_g for the duration of the fire endurance test.

Even though the performance of FRP-strengthened concrete members at normal temperature is acceptable,

information about their performance at elevated temperatures is limited. The objective of this study is to examine the effect of elevated temperature on behavior of RC circular columns strengthened with different FRP systems. To achieve this goal, unstrengthened as well as FRP-strengthened column specimens were prepared and then subjected to ambient temperature and high temperature regimes of 100, 200, 300, 400, 500, and 800°C for a period of 3 h. Thereafter, they were left to cool down at room temperature and then tested under axial compression until failure.

It should be noted that the main purpose of this research is to study the residual strength and stiffness of both unstrengthened and FRP-wrapped RC columns after their exposure to high temperature and not during elevated temperature exposure. For unstrengthened columns, the residual capacity can be used for repair and strengthening purposes. For FRP-wrapped columns, the residual strength can be used to assess FRP effectiveness in preserving the axial load capacity after high temperature exposure and also for the rehabilitation of heat damaged FRP-wrapped columns. Also, FRP composites may be used to provide passive confinement in case of strengthening for extreme or infrequent load events such as seismic retrofit of RC columns. The FRP confinement will remain in an unstressed state until the extreme event unfolds. Because FRP composite systems are used as secondary reinforcement in this case, there is a low probability of elevated temperatures occurring simultaneously with an extreme loading event unless the event caused the elevated temperatures. Therefore, this study focused on whether the composite reinforcing system is still effective as secondary reinforcement after cooling and what effect the heat treatment has on the mechanism of failure. Accordingly, columns were unstressed while being heated and the axial preloading that simulates the service load level was not used in this study. This was done to assure that the columns would not fail under a long duration of high temperature exposure, and hence be able to assess their residual capacity.

Experimental program

In this test program, 32 RC circular columns were cast and subjected to high temperatures ranging from 100 to 800°C. When cast, all columns were identical having a diameter of 242 mm and a length of 900 mm. All columns were reinforced with 4ϕ10 mm longitudinal steel bars, which were tied in the transverse direction using ϕ6 mm bars at a center-to-center spacing of 200 mm as shown in Figure 1(a). This longitudinal reinforcement resulted in a reinforcement ratio of 0.68%, which is less than the minimum reinforcement of 1% for RC columns stipulated in the ACI 318-14 code requirements.[26] The reduced reinforcement ratio was selected on purpose to account for the loss in steel reinforcement area as a result of steel corrosion in the harsh environment of the coastal regions of Saudi Arabia. Details about strengthening schemes used and the heating regimen are provided in the following sections.

Test matrix

Table 1 provides the test matrix for the columns to be used for this study. As shown in the table, the columns were cast in three groups. It should be noted that each column was duplicated to confirm the repeatability of the results and to get more certitude in the outcomes of this research. The group I.D "C" comprised of 14 unstrengthened columns, whereas the group I.D "CF" and "GF" comprised of 14 and 4 columns strengthened with CFRP and GFRP laminates, respectively. Two columns from each group were tested at room temperature and were considered as control specimen for their respective groups. All other columns were tested at elevated temperatures as indicated in the table. Out of the 14 CFRP-strengthened specimens, 4 columns were insulated before subjecting them to elevated temperatures, using a locally available insulation material. As shown in Figure 1(b), a single layer of CFRP (or GFRP) sheet was used to strengthen the columns and the sheet was bonded to concrete surface with the fibers oriented in the hoop direction.

Specimen preparation

Reinforcement cage as per design was first prepared and plastic pipe framework was used to cast concrete for columns as shown in Figure 2(a). Proper compaction of concrete was achieved using pin-type vibrator. All columns were cast using the same batch of ready-mix concrete to avoid any material variations. Standard six 150 mm × 300 mm cylinders were also cast to be tested for measuring the compressive strength of concrete. Figure 2(b) shows all column specimens after casting and leveling of concrete.

The FRP sheets were applied 1 month after concrete casting. Before the application of FRP sheets, the RC columns were ground using sand paper and sand blasted to prepare the concrete surface, to make sure it is dry and free of dust and laitance. It is then treated with a cloth dipped in acetone. The resin-based epoxy is then applied in a thin layer over the concrete surface. The FRP sheets were then saturated using approved saturation methods of the manufacturer. Care was taken to make sure the epoxy was distributed uniformly over the FRP sheets. Once fully saturated by epoxy, the FRP layers are then bonded to the surface of the column. All voids between the concrete surface and the sheet

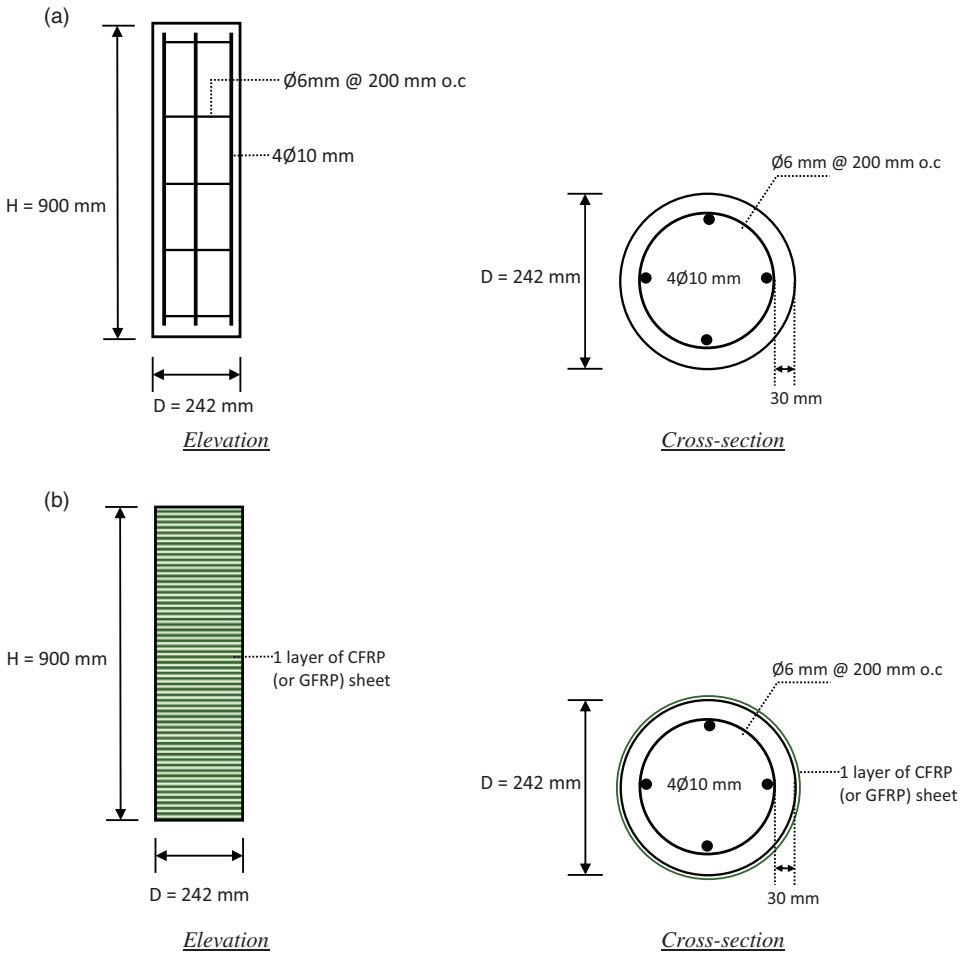

Figure 1. Details of test specimens. (a) Unstrengthened specimens and (b) FRP-strengthened specimens.

are removed carefully by hand. The FRP sheets had the fibers oriented in the hoop direction with an overlap of 150 mm. The columns were then kept under laboratory conditions until full curing of epoxy was achieved, which was suggested as 72 h by the manufacturer. Figure 2(c) shows the columns after strengthening using both CFRP as well as GFRP sheets.

The insulation of the columns was carried out as per the manufacturer's recommendation by using a minimum thickness of 40 mm and applying the material using a spray concrete system. Prior to application, the CFRP surface was prepared by cleaning and removing all carbon dust from the surface. The composite surface was then primed using epoxy resin, over which the fire-resistant mortar was then wet sprayed. Figure 2(d) shows a CFRP-strengthened column after the insulation process is completed.

Material properties

Concrete. Ready-mix concrete having a cement content of 400 kg/m^3 was used for casting the RC column specimens. The maximum size of the aggregate used was 10 mm. The specified compressive strength measured as per ASTM C39M[27] at the time of the test was 42 MPa. The concrete mix proportions are detailed in Table 2.

Reinforcement bars. Locally manufactured ribbed steel rebars were acquired for the longitudinal as well as tie reinforcement. Tensile tests were conducted according to ASTM E8/E8M[28] on both ϕ10 mm as well as ϕ6 mm bars and the average yield strength was measured to be 593 MPa and 301 MPa, respectively.

FRP laminate. For CFRP laminate used in this study, unidirectional carbon fabric was used. The epoxy used in the laminate was a two component resin-based epoxy and was mixed in a ratio of 100: 34.5 by weight. Tables 3 and 4 enlist the properties for the CFRP composite gross laminate and the epoxy adhesive, respectively. Gross laminate properties are based on standard coupon tests carried out in accordance with ASTM D3039/3039M.[30] For GFRP laminate

Table 1. Summary of test matrix.

Group ID	Specimen ID	Strengthening system		Temperature (°C)	Exposure time (h)	Thermal insulation	No. of specimens
		No. of layers	Type				
C	C-R	Unstrengthened		Room temp. (26°C)	–	No	2
	C-100	Unstrengthened		100	3	No	2
	C-200	Unstrengthened		200	3	No	2
	C-300	Unstrengthened		300	3	No	2
	C-400	Unstrengthened		400	3	No	2
	C-500	Unstrengthened		500	3	No	2
	C-800	Unstrengthened		800	3	No	2
CF	CF-R	1	CFRP	Room temp. (26°C)	3	No	2
	CF-100	1	CFRP	100	3	No	2
	CF-200	1	CFRP	200	3	No	2
	CF-300	1	CFRP	300	3	No	2
	CF-400	1	CFRP	400	3	No	2
	CF-500-IN	1	CFRP	500	3	Yes	2
	CF-800-IN	1	CFRP	800	3	Yes	2
	GF-R	1	GFRP	Room temp. (26°C)	–	No	2
	GF-200	1	GFRP	200	3	No	2
Total no. of specimens							32

used in the study, a custom weave unidirectional glass fabric was used along with the same epoxy. Material properties for the GFRP composite gross laminate are also listed in Table 3.

Insulation material. The insulation material used in the study was locally available Sikacrete-213F, which is cement-based dry-mix fire protection mortar. It is specifically designed to protect FRP-strengthened surfaces from elevated temperatures or fire. Manufacturer provided properties of the material have been presented in Table 5.

Heating regimen for columns

The heating of the columns was started after a period of 60 days of pouring the concrete and 1 month after the FRP installation. An electric furnace with internal dimensions of 1 m × 1 m × 1 m was used for this purpose. As shown in Figure 3 at a time, three to four columns in an unstressed state were heated as per the heating schedule described in the test matrix. The oven walls were protected from explosive spalling of concrete at high temperatures by having a protection wall around the columns. Individual time-temperature curves used in the study for each temperature exposure are shown in Figure 4. The approximate heating rate of the oven was in the range 5–15°C/min. Also shown in Figure 4 is the standard temperature versus time curve (ISO 834) used for structural fire resistance testing in Europe.[31] It is clear from the figure that the oven used in the current study was unable to achieve rapid heating rates that are representative of the standard fire. However, this is not considered critical because the current study is concerned primarily with confinement of concrete within a column's core using FRP composites (i.e. inside the hoop ties or spirals). Within the core concrete, the heating rates and peak temperatures experienced would be moderated by the thermal protection of the cover concrete, and would likely be similar to the exposures reproduced by the heating profiles imposed herein. It should also be noted that the standard fire does not necessarily reflect the actual heating of concrete within a real structure during a real fire.

The exposure time for all columns in this study was kept as 3 h. Because of the small column diameter of 242 mm, the 3 h duration was found to be the time required for the heat to transfer from the oven to the centerline of each test column and hence the temperature at the center of each column would reach its target value. The 3 h period has kept the specimens being exposed to temperatures in excess of T_g of the epoxy for at least 4 h duration, including rise-up from room temperature, constant temperature for 3 h, and gradual

Figure 2. Specimen preparation, strengthening and insulation. (a) Plastic pipe formwork and steel cage during casting; (b) column specimens after concreting and leveling in plastic pipe framework; (c) columns ready for curing after FRP application; and (d) column insulated using Sikacrete-213F.

Table 2. Proportions of ingredients used for concrete mix.

Ingredients	Quantity (for 1 m^3)
Cement (Type I)	400 kg
Silica sand	585 kg
Washed sand	195 kg
10 mm aggregate (3/8″)	315 kg
20 mm aggregate (3/4″)	735 kg
Water	170 kg
Admixture	0.3% by weight of cement

Table 3. Properties of FRP systems used in this study[a].

Property	CFRP system	GFRP system
Thickness per layer (mm)	1	1.3
Ultimate tensile strength (MPa)	846	552
Ultimate tensile strain	1.10%	1.90%
Tensile modulus of elasticity (GPa)	77.28	27.6

[a]Based on standard test coupons.

Table 4. Properties of epoxy adhesive used in this study[a].

Adhesive property	Value
Tensile strength (MPa)	71.6
Tensile modulus of elasticity (GPa)	1.862
Tensile strain at break	5.25%
Glass transition temperature, T_g (°C)	85
Thermal decomposition temperature[b], T_d (°C)	345

[a]Based on manufacturer's datasheet.
[b]Obtained from Khalifa.[29]

Table 5. Properties of insulation material Sikacrete-213F[a].

Material property	Value
Layer thickness (mm)	40
Compressive strength (MPa)	2.0
Thermal conductivity (W/mK)	0.23

[a]Based on manufacturer's datasheet.

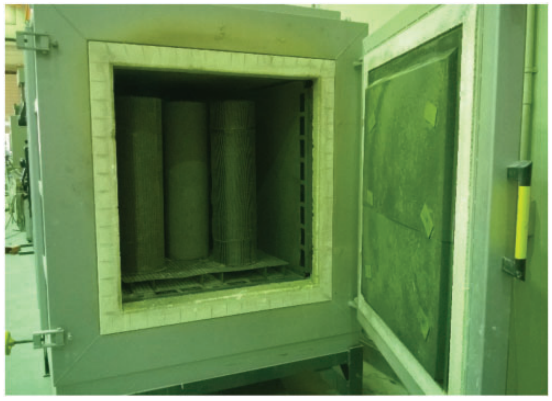

Figure 3. Oven with specimens ready for heating.

cool-down to ambient (see Figure 4); thereby subjecting the columns to severe heating regimes of high temperature for long period. The oven temperature is monitored automatically with an in-built thermocouple, which provides its feedback to a digital read-out of the oven controller. Once the exposure time was reached, the oven would automatically shut down and the temperature was allowed to fall down. The columns were then allowed to cool down naturally within the oven. The door of the oven was permitted to be opened only when the temperature inside the oven is reduced to 200°C for cases where the columns were subjected to even higher temperatures. After cooling down, the columns were removed from the oven and kept at room temperature in the laboratory until testing.

At temperatures of 100, 200, and 300°C, no visible damage was observed in the unstrengthened column specimens. However at 400, 500, and 800°C concrete appeared to be darkened as a result of heating as shown in Figure 5. Some cracks were also observed on the surface. Similar observations were reported by Freskakis et al.[32] for concrete under high temperature exposure. For the CFRP- and GFRP-wrapped columns subjected to 100 and 200°C, the epoxy appeared to melt while the columns were in the oven, however, post-cooling the epoxy regained its original form. Comparable observations were made in another study by the authors.[19] For the CFRP-strengthened columns, the CFRP composite was found to be charred at 300 and 400°C but still adhered to the concrete surface. Figure 6 shows the insulated CFRP-wrapped columns after being subjected to 500 and 800°C. The insulation was effective in protecting the column subjected to 500°C and the CFRP appeared to be undamaged. However, the insulated CFRP-strengthened column subjected to 800°C had visible charring of the composite strands. No de-bonding was observed in either of the insulated columns. The same observation was made in some other studies by Chowdhury et al.[22] and Cree el al.[23] in which insulated FRP-strengthened RC columns were subjected to standard fire tests.

Test procedure

The instrumentation layout and test setup for the experimental testing of the RC columns is shown in Figure 7. All columns were tested under uniaxial compression using an AMSLER compression testing machine with a maximum compression capacity of 10,000 kN. A displacement controlled rate of loading of 0.5 mm/min was used for the test. Prior to the tests, all columns were capped at the base and the top ends using gypsum capping to make sure fully concentric uniform loading over the entire column surface is achieved. To avoid local failure due to stress-concentration, the top and bottom 150 mm length of the columns were restrained in the hoop direction using three layers of CFRP sheet as shown in Figure 7. The load applied to the columns was measured using a built-in load cell of the AMSLER testing frame. The instrumentation of the columns comprised of two linear variable displacement transducers (LVDT) on opposite ends, measuring the axial deformation in the columns within a gauge length of 300 mm in the middle-third length of the column. Two strain gauges were attached at mid-height, on opposite faces of the columns in axial direction to measure the axial strains and another two strain gauges were attached at the same locations but, in the lateral direction to measure column surface lateral strains. All data were recorded via a data acquisition system at intervals of 1 s.

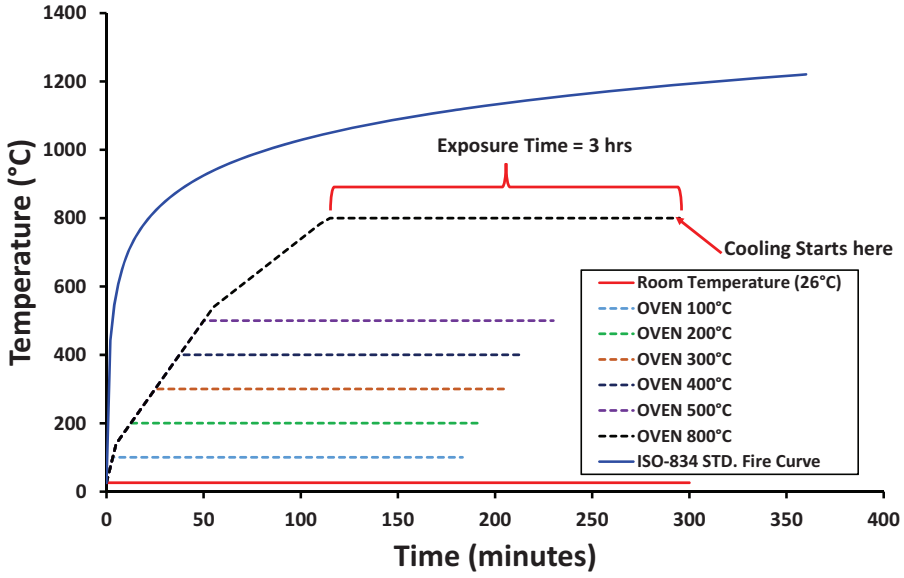

Figure 4. Time-temperature curves used in the study.

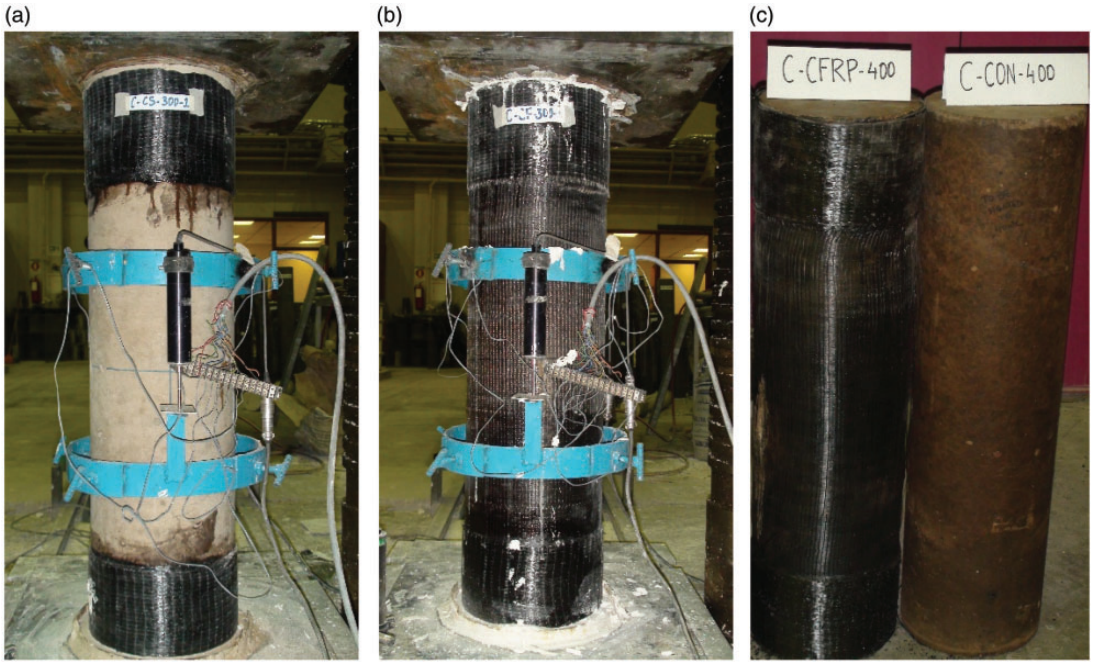

Figure 5. Columns subjected to an elevated temperature for 3 h. (a) Unstrengthened column subjected to 300°C; (b) CFRP-strengthened column subjected to 300°C; and (c) control and CFRP-wrapped columns subjected to 400°C.

Test results and discussion

Modes of failure

All specimens were tested under uniaxial compression until failure. A typical crushing mode of failure was noticed for all specimens. All columns failed at mid-height as a result of restraining the top and bottom ends of the columns using CFRP sheets, which resulted in transferring the stresses to the middle third of the column. For the unheated unstrengthened columns, failure started typically by crushing of concrete followed by its brittle and

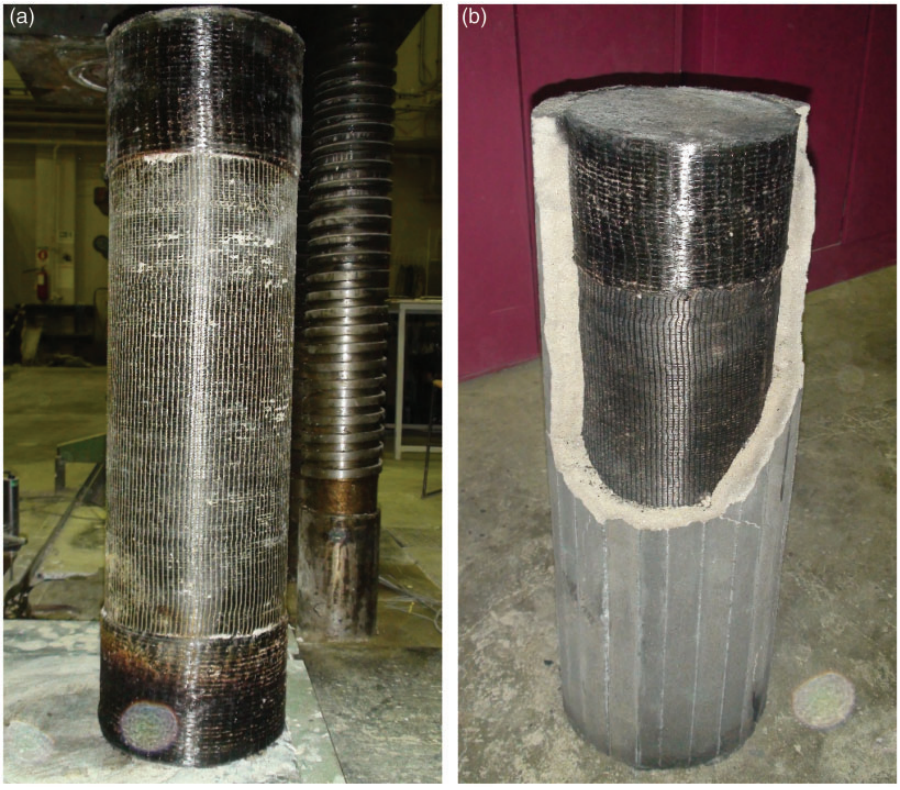

Figure 6. Insulated CFRP-strengthened columns after exposure for 3 h. (a) Insulated CFRP-wrapped column exposed to 500°C and (b) insulated CFRP-wrapped column exposed to 800°C.

explosive spalling. Further loading resulted in complete spalling of concrete thereby exposing the steel bars, which were found to be bent at mid-height or thereabouts. It was noticed that all four steel bars were bent in a similar pattern indicating uniform concentric application of the load. For the heated unstrengthened columns, a far less explosive and a more ductile failure was observed. However, the failure mode remained the same as shown in Figure 8.

For columns strengthened with CFRP sheets, a cracking noise was observed prior to failure, which was accompanied by a reduction in load carrying capacity of the column. Concrete crushing then took place which was followed by tearing of the FRP material. The final failure was explosive and resulted in a loud noise due to sudden release of energy and was characterized by complete rupture of the CFRP sheet at mid-height location. Figure 9 shows typical failure modes for CFRP-strengthened unheated and heated columns. For columns strengthened with GFRP sheets, the failure mode was very similar to the CFRP-wrapped specimens, except that the final failure was far less explosive compared with the CFRP-strengthened specimens. The same cracking noise was observed at the beginning of the failure indicating activation of the jacket providing the uniform confinement. The typical modes of failure for the GFRP-strengthened columns have been depicted in Figure 10.

Stress–strain curves

The average axial stress plotted versus axial and lateral strains for unstrengthened, CFRP- and GFRP-strengthened specimens is shown in Figures 11 to 13, respectively. The average axial stress was calculated by dividing the axial load by the gross cross-sectional area of the column. The axial strains were obtained by dividing the average axial displacement as given by the LVDTs by the gauge length. It should be noted that readings of the vertical strain gauges were only used to confirm the axial strain calculated from the LVDTs and they were not used for plotting the stress–strain curves of test specimens. The reason is that these gauges get severely damaged once the FRP jacket ruptures and their readings for the descending part of the curves are then lost. The lateral strains were measured directly using the horizontal strain gauge sensors. Figure 11 shows the stress–strain curves for unstrengthened columns at room and elevated temperatures. As seen from the figure, the peak axial stress for columns gradually

decreases with the increase in exposure temperature. However, the axial strain at peak load, the peak axial strain as well as the peak lateral strain increase significantly after temperature exposure, indicating a more ductile behavior for columns subjected to elevated temperatures. This decrease in the axial strength and the increase in peak axial and lateral strains in comparison with unheated specimens was more pronounced for specimens subjected to temperatures of 300°C and upwards, compared with specimens subjected to temperatures of 100 and 200°C. In general, a reduction in column stiffness was noticed for all unstrengthened columns subjected to elevated temperatures.

Figure 7. Instrumented column ready for testing.

Figure 12 shows the stress–strain curves for CFRP-strengthened specimens at room and elevated temperatures for both insulated as well as uninsulated specimens. As seen from the figure, a marked reduction was noticed in the axial strength for columns at elevated temperatures (100–400°C) compared with the column at room temperature. In case of CFRP-wrapped specimens, the axial strains at peak load, peak axial strains, and the peak lateral strains, all decreased with the increase in the exposure temperature (100–400°C). A general reduction in stiffness of the columns was also observed with the increase in exposure temperature.

Figure 13 shows the stress–strain curves for the two GFRP-strengthened specimens. As seen from the figure, exposure to an elevated temperature of 200°C resulted in a reduction of axial strength, peak axial strain, as well as the peak lateral strain values. However, for the GFRP-strengthened specimens, the axial strain at peak load increased for the specimen subjected to an elevated temperature in comparison with the specimen at room temperature.

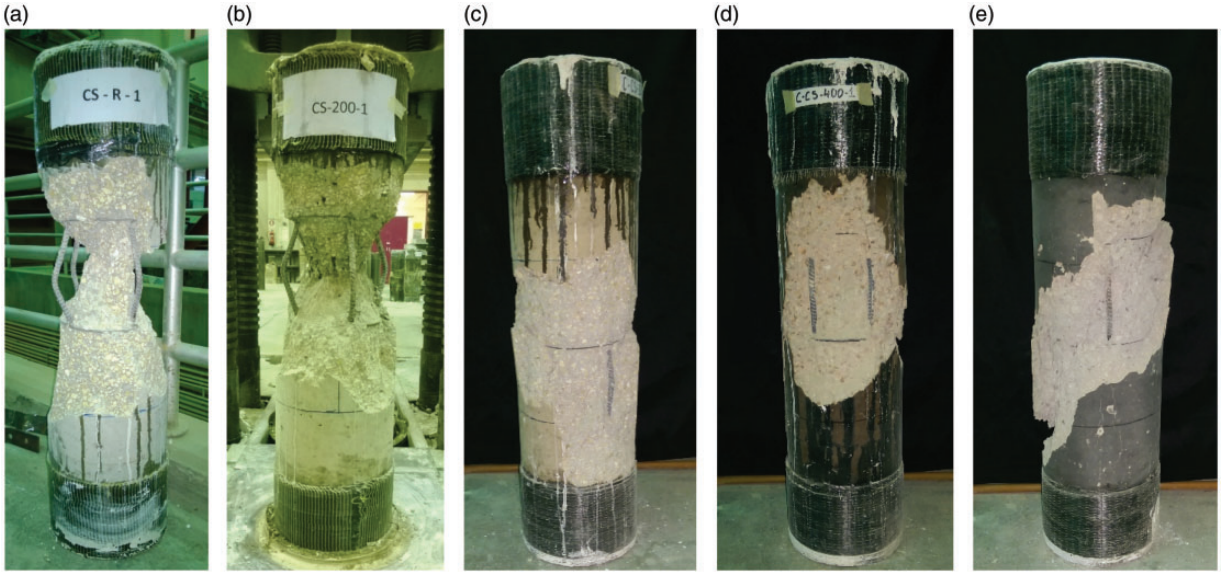

Figure 8. Typical failure modes for unstrengthened specimens. (a) Room Temp.; (b) 200°C; (c) 300°C; (d) 400°C; and (e) 800°C.

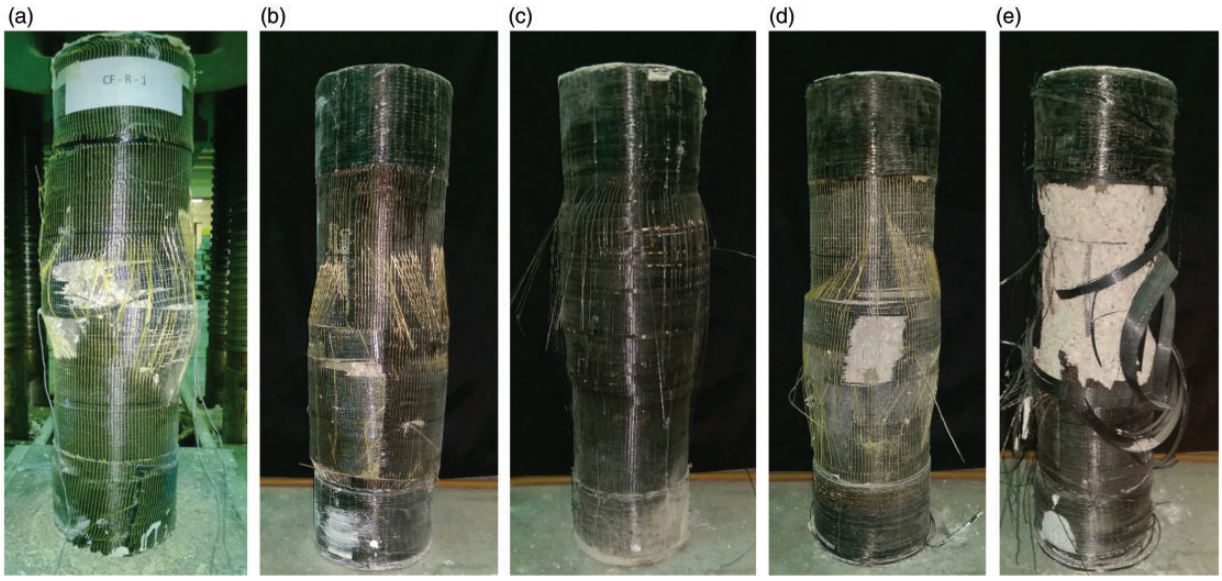

Figure 9. Typical failure modes for CFRP-strengthened specimens. (a) Room Temp.; (b) 300°C; (c) 400°C; (d) 500°C insulated; and (e) 800°C insulated.

Figure 10. Typical failure modes for GFRP-strengthened specimens. (a) Room Temp. and (b) 200°C.

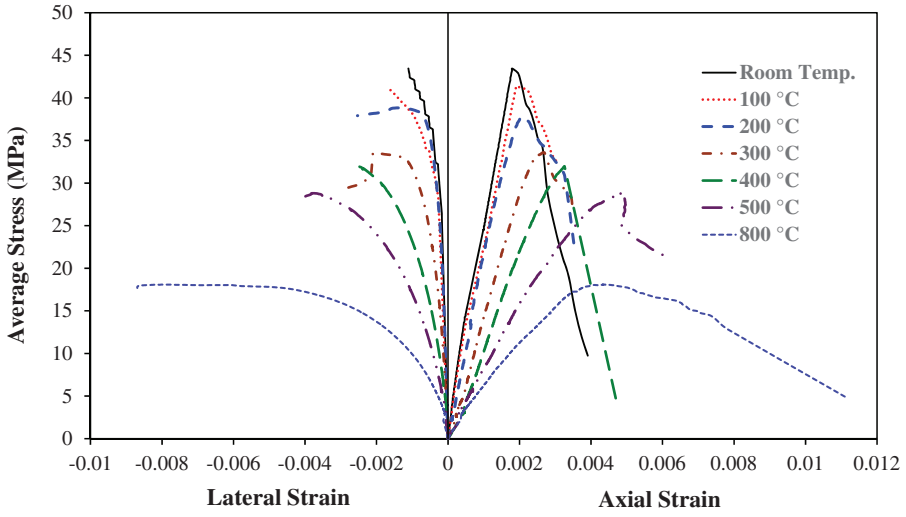

Figure 11. Stress–strain curves for unstrengthened specimens.

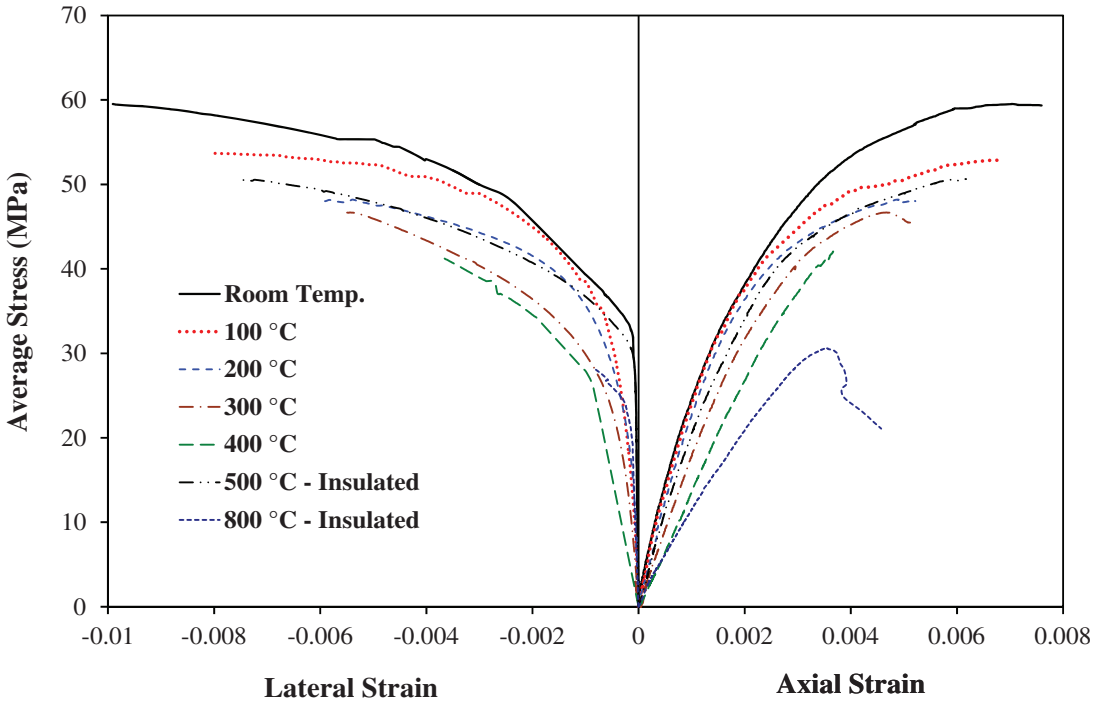

Figure 12. Stress–strain curves for CFRP-strengthened specimens.

Effect of elevated temperature exposure

Table 6 presents a summary of experimental results for all columns tested in this study. Results are presented in terms of peak axial load, secant stiffness at service load, the peak average and actual axial stresses, and the peak strains in axial and lateral directions. It should be noted that the test results of the repeated columns were close to each other and the values enlisted in Table 6 are the average of the two specimens. In this study, the secant stiffness at service load is defined as the ratio of service compressive axial load to the axial displacement at that load as shown in Figure 14. The service load was considered to be 40% of the ultimate axial load. The peak average concrete stress reported in Table 6 is obtained by dividing the peak axial load by the cross-sectional area of the column. However, the peak actual concrete stress enlisted in Table 6 was calculated from the

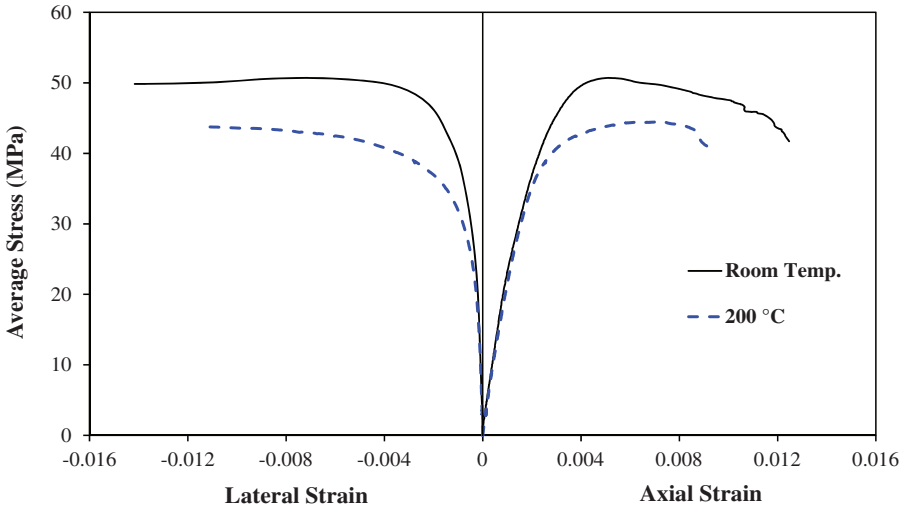

Figure 13. Stress–strain curves for GFRP-strengthened specimens.

Table 6. Experimental results for columns tested in this study.

Group ID	Specimen ID	Peak axial load (kN)	Secant stiffness at service load (kN/mm)	Concrete compressive strength (MPa)		Axial strain at peak stress	Peak axial strain	Peak lateral strain
				Peak average stress	Peak actual stress			
C	C-R	1982	1407	43.1	39.3	0.0018	0.0039	0.0011
	C-100	1901	1244	41.3	37.5	0.0019	0.0030	0.0017
	C-200	1765	1157	38.4	34.6	0.0023	0.0035	0.0025
	C-300	1545	725	33.6	29.8	0.0027	0.0035	0.0026
	C-400	1471	563	32.0	28.1	0.0033	0.0033	0.0030
	C-500	1325	399	28.8	24.9	0.0049	0.0062	0.0040
	C-800	832	252	18.1	14.1	0.0045	0.0112	0.0087
CF	CF-R	2669	1267	58.0	54.4	0.0073	0.0076	0.0092
	CF-100	2431	1232	52.9	49.1	0.0068	0.0068	0.0081
	CF-200	2217	1141	48.2	44.5	0.0049	0.0052	0.0059
	CF-300	2146	879	46.7	42.9	0.0047	0.005	0.0055
	CF-400	1934	694	42.1	38.3	0.0037	0.0037	0.0037
	CF-500-IN	2329	1007	50.6	46.9	0.0062	0.0062	0.0076
	CF-800-IN	1410	519	30.7	26.8	0.0035	0.0046	0.0008
GF	GF-R	2332	1228	50.7	47.0	0.0051	0.0125	0.0142
	GF-200	2047	1111	44.5	40.7	0.0073	0.0093	0.0115

following equation, which is based on the ACI 318-14 code[26] and the ACI 440.2R-08 guidelines.[33]

$$\text{Peak actual concrete stress} = f'_{cc,T} = \frac{P_u - A_{st}f_y}{A_g - A_{st}} \quad (1)$$

where P_u = peak axial load; A_{st} = area of longitudinal steel bars; f_y = yield strength of longitudinal steel; and A_g = gross area of column section. Effect of elevated temperature exposure on behavior of unstrengthened and strengthened specimens are discussed below.

Unstrengthened columns. Figure 15(a) and (b) shows the percentage loss in the axial strength and secant stiffness, respectively, for specimens at elevated temperatures in comparison with specimens at room temperature for unstrengthened columns. As seen from Table 6 and Figure 15(a) and (b), the percentage loss in axial

strength and secant stiffness is more pronounced for specimens subjected to temperatures above 300°C. This observation is consistent with previous research on the residual properties of fire-exposed concrete.[32]

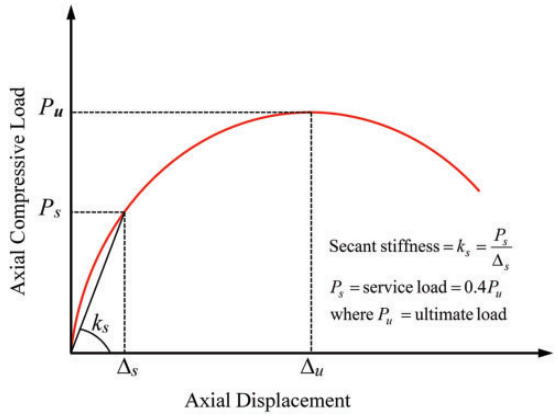

Figure 14. Definition of secant stiffness.

It was noticed that the loss of compressive strength and secant stiffness after being exposed to 400°C for 3 h duration was about 26% and 60%, respectively, as seen in Figure 15(a) and (b). However, in the test carried out by Chowdhury et al.,[22] it was observed that even though the temperature at the concrete surface for the insulated column went up to approximately 400°C at 5 h, the column still maintained a constant axial deformation value under the sustained applied load. The difference between unstrengthened specimens tested in this research and columns tested by Chowdhury et al.[22] is that the rate of temperature increase was much severe in this study (temperature increased to 400°C in about 40 min and was maintained constant for the next 3 h), however, in the study by Chowdhury et al.,[22] the temperature at concrete surface gradually increased to 400°C in 5 h. This leads to the conclusion that the rate of temperature increase plays an important role in the performance of concrete under elevated temperature regimes. For the same target temperature, as the rate of temperature rise increases the loss in concrete strength becomes more pronounced.

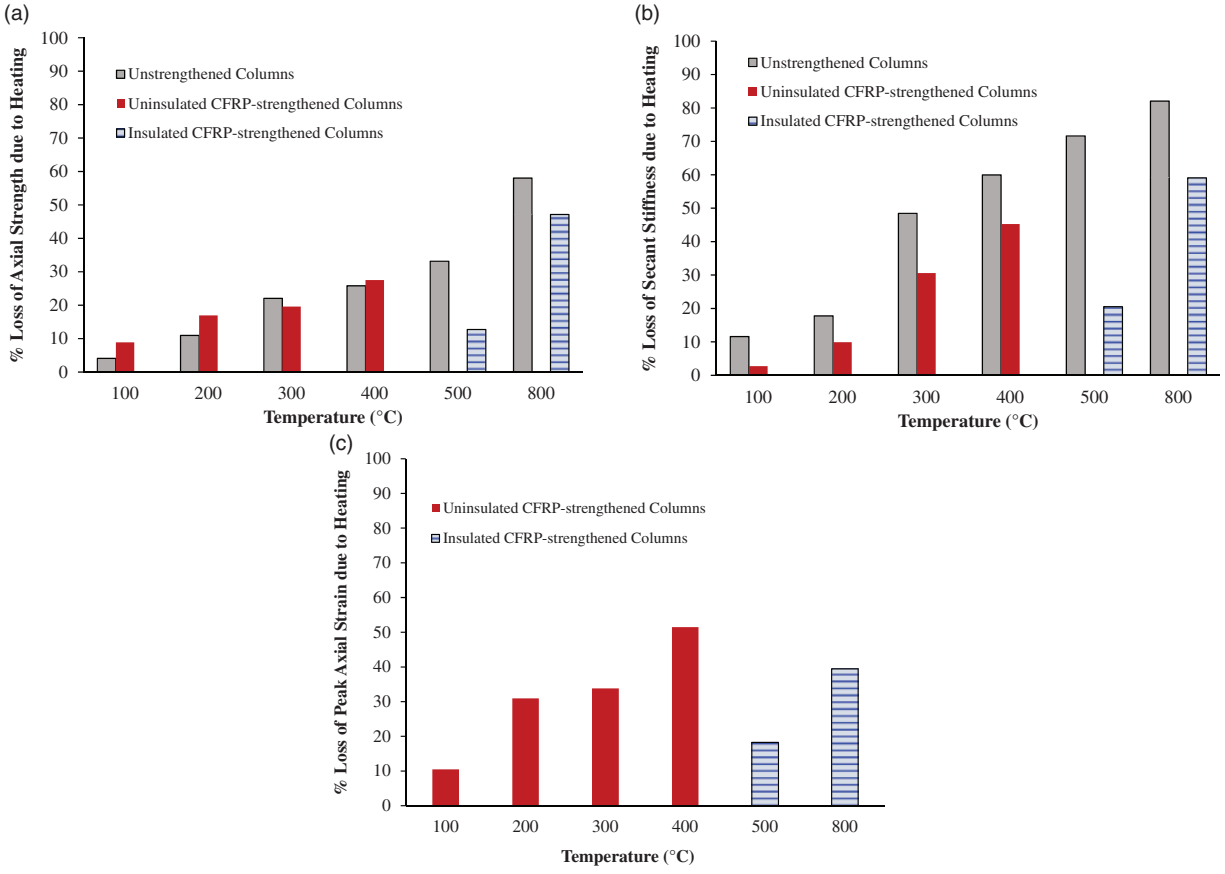

Figure 15. Effect of exposure temperature on percentage loss of strength, stiffness, and peak strain of test specimens. (a) % Loss of axial strength, (b) % loss of stiffness and (c) % loss of peak axial strain.

The percentage losses in axial strength for specimens subjected to 500 and 800°C are 33 and 58%, respectively; whereas the percentage loss in secant stiffness for the same specimens is 72 and 82%, respectively. This steep reduction could be attributed to the fact that as the exposure temperature increases, the concrete becomes soft and loses the internal mix water thereby making it more porous. It should also be noted that for columns exposed to higher temperatures, the exposure time to an elevated temperature is also increased thereby attributing to a higher deterioration in concrete strength.

CFRP-strengthened columns. Figure 15(a) to (c), respectively, shows a comparison of percentage loss in axial strength, secant stiffness, and the peak axial strain values for uninsulated as well as insulated CFRP-strengthened specimens in comparison with a strengthened column at room temperature. As seen from the figures, for all CFRP-wrapped columns an increase in percentage loss in all measured response parameters was noticed with the increase in exposure temperature. For uninsulated CFRP-strengthened columns tested in this study, it was found out that after being exposed to high temperature of 300°C (about 3.5 T_g) sustained for 3 h duration, the ultimate capacity of the strengthened column was about 139% of that for unstrengthened column exposed to the same heating regime. It is to be noted that even for a CFRP-confined specimen subjected to 400°C, which is almost $5T_g$, the axial stress capacity is 31.5% greater compared with the unstrengthened specimen subjected to the same temperature, whereas its axial stress capacity is 98% of that of the unstrengthened specimen at room temperature. This could be attributed to the fact that the presence of a CFRP layer around concrete has resulted in the concrete being protected from the exposure to heat thereby, even though the effect of strengthening had deteriorated but the concrete load-carrying capacity was unaffected. However, compared with the CFRP-strengthened specimen at room temperature, the axial stress for the specimen subjected to an elevated temperature of 400°C was reduced by 27.5%. This supports the conclusion that as long as the temperature at the FRP level is still under the decomposition limit of the epoxy polymer matrix (345°C in this study), the FRP is deemed effective (but with less efficiency) in contact-critical applications. The same conclusion was reached by Foster and Bisby[34] as it was stated that for FRP strengthening applications that are not bond critical, much smaller thicknesses of supplemental insulation may be allowable for FRP-strengthened concrete members (and their residual performance may be much better than currently thought). Contrary to this conclusion, Chowdhury et al.[22] mentioned that if the temperature at the FRP level exceeds T_g, it can be conservatively assumed that the FRP wraps are rendered structurally ineffective.

Effect of insulation

As seen from Figure 15 and Table 6, the effect of insulation of CFRP-wrapped specimens is pronounced in terms of retaining the axial strength capacity, especially for the insulated specimen subjected to 500°C. As seen from the stress–strain curve in Figure 12, the behavior of the insulated column subjected to 500°C is enhanced in terms of axial strength, compared with uninsulated CFRP-wrapped specimens subjected to 300 and 400°C. The behavior of the insulated column subjected to 500°C is comparable with an uninsulated CFRP-strengthened column subjected to 200°C in terms of its load carrying capacity. This depicts that insulation could be very effective in preventing the heat induced damage to CFRP-strengthened columns up to certain temperatures and exposure periods. The insulated column subjected to 800°C, had a marked reduction in its axial stress capacity compared with CFRP-confined specimens subjected to other temperatures. However, compared with the unstrengthened specimens exposed to the same temperature of 800°C, the axial stress capacity of insulated CFRP-strengthened column was almost 70% higher. This indicates that the insulation was effective to some extent in minimizing the damaging effects of the elevated temperatures from reaching the concrete core. The same conclusion was supported in the standard fire tests conducted by Chowdhury et al.,[22] whereas in their study, the insulated FRP-wrapped column failed at a higher applied load than the uninsulated column because the supplemental fire protection system used was able to maintain low temperatures in the concrete and reinforcing steel during the fire tests, thus enabling the concrete and steel to retain most of their room temperature strength during the fire endurance tests.

When RC columns are strengthened using externally bonded FRP composites, their ultimate capacity increases, hence allowing for higher service loads to be applied. Under high temperature exposure, the ultimate capacity of the FRP-wrapped column gets reduced with increasing temperature and failure of the column would arise when its ultimate capacity becomes less than the applied service load. As a result, for safety at fire or high temperature exposure, the ultimate capacity of the FRP-upgraded column should stay greater than its applied service load for the required duration of fire or high temperature.[35] Figure 16 shows the variation of compressive strength enhancement ratio with exposure temperature. Compressive strength enhancement ratio is defined as the ratio of confined

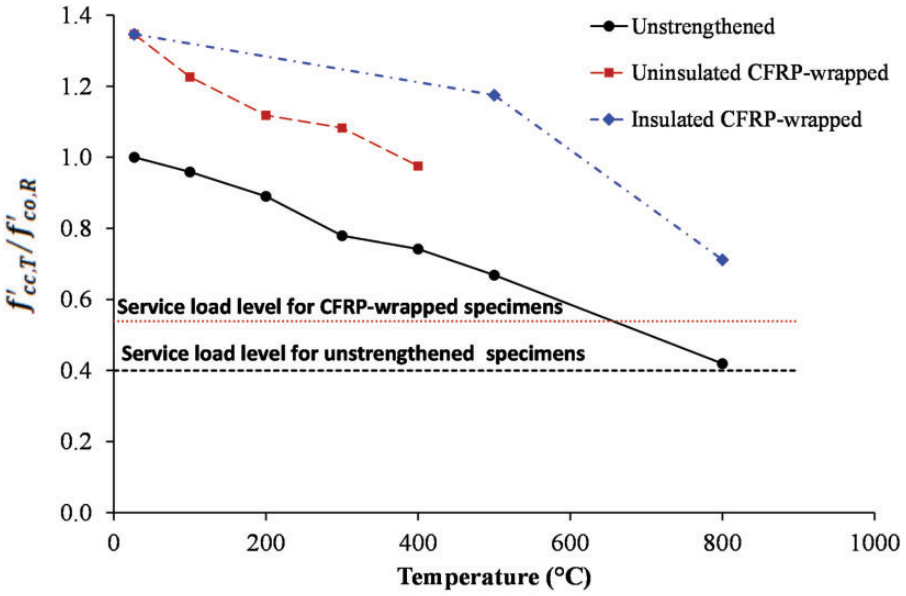

Figure 16. Variation of compressive strength enhancement ratio with exposure temperature.

compressive strength after exposure to elevated temperature ($f'_{co,T}$) to the unconfined compressive strength at room temperature ($f'_{co,R}$). From the figure, it is depicted that as a result of insulation of CFRP-strengthened specimens, even exposing the specimen to a temperature of 800°C for 3 h has kept the enhancement ratio above the service load level for strengthened specimen, thereby demonstrating its effectiveness in preventing the column collapse at this level of temperature exposure.

Effect of FRP type

Figure 17 shows a comparison between the two types of strengthening systems in terms of axial strength, secant stiffness, and the peak axial strain. As seen from the figure, for an elevated temperature exposure of 200°C, the percentage loss in the three parameters compared with the specimen at room temperature, is more pronounced in case of CFRP system. This surprising finding could be attributed to the fact that the voids within the strengthening fabric play an important role in the transmittal of the heat to the epoxy matrix. As seen in Figure 18, which shows a close-up view of both carbon and E-glass fibers used in this study, the voids in the E-glass fibers are almost invisible and are covered-up by the custom fabric weave, whereas the voids in carbon fibers are visibly bigger. These voids may bring the epoxy matrix to be directly subjected to the detrimental effects of the high temperatures resulting in degradation in its strength. Nevertheless, in case of GFRP sheet, the nonappearance of voids in between the glass fibers may safeguard the epoxy matrix from the hostile effects of the high temperatures.

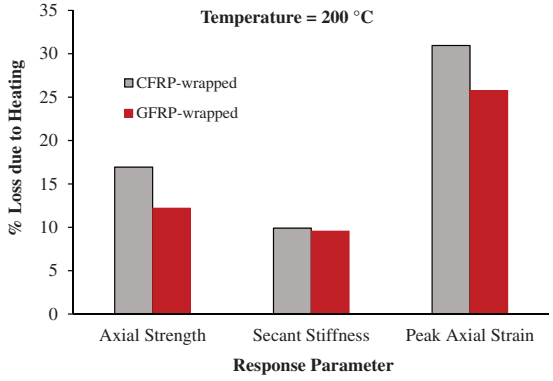

Figure 17. Performance comparison between CFRP- and GFRP-strengthened specimens at 200°C exposure.

Design aspects in light of ACI 440.2R-08 guidelines

As per the ACI 440.2R-08 guidelines,[33] the maximum compressive strength for FRP-confined concrete at room temperature $f'_{cc,R}$ is given by the following equation:

$$f'_{cc,R} = f'_{co,R} + 3.3\psi_f k_a f_l \text{ (MPa units)} \quad (2)$$

This equation was modified in this study to include the effect of high temperature exposure by the inclusion of a new strength reduction factor (ψ_T) as follows:

$$f'_{cc,T} = f'_{co,R} + 3.3\psi_T\psi_f k_a f_l \text{ (MPa units)} \quad (3)$$

where $f'_{cc,T}$ = confined compressive strength after exposure to elevated temperature; $f'_{co,R}$ = unconfined

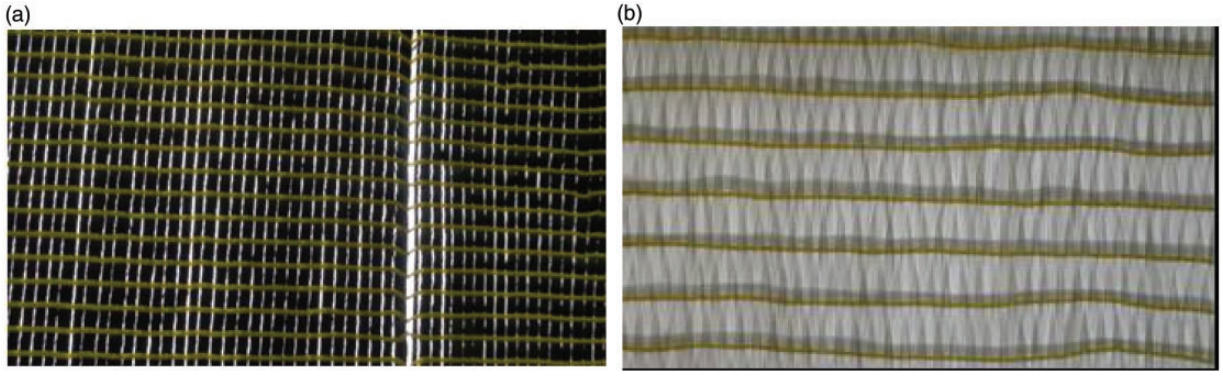

Figure 18. Close-up picture of carbon and E-glass fibers used in this study. (a) Visible voids between carbon fibers and (b) invisible voids between E-glass fibers.

compressive strength at room temperature; ψ_T = FRP strength reduction factor due to elevated temperature exposure; ψ_f = FRP strength reduction factor = 0.95; k_a = efficiency factor accounting for section geometry = 1.0 for circular columns; and f_l = maximum confinement pressure given by

$$f_l = \frac{2E_f n t_f \varepsilon_{fe}}{D} \tag{4}$$

where E_f = tensile modulus of elasticity of FRP material; n = no. of plies of FRP reinforcement; t_f = thickness of one ply of FRP reinforcement; ε_{fe} = effective strain level in the FRP at failure = 0.55 × strain at rupture of the FRP reinforcement; and D = column diameter. By substituting equation (2) into equation (3), the latter can be rewritten as

$$f'_{cc,T} = f'_{co,R} + \psi_T (f'_{cc,R} - f'_{co,R}) \tag{5}$$

The FRP strength reduction factor due to elevated temperature exposure can be then expressed as

$$\psi_T = \frac{f'_{cc,T} - f'_{co,R}}{f'_{cc,R} - f'_{co,R}} \tag{6}$$

Besides the test results of this study, the experimental data of 48 uninsulated FRP-strengthened circular concrete specimens subjected to different heating regimes were collected from the literature and are presented in Table 7. Similar to the test columns of this study, all FRP-strengthened specimens of Table 7 were first exposed to elevated temperature environments and then left to cool down at room temperature. Subsequently, they were tested under axial compression until failure. With the inclusion of the seven uninsulated FRP-strengthened columns of this study, the whole database incorporates results of 55 specimens under different elevated temperature exposure. Using the dataset of the 55 uninsulated FRP-strengthened specimens, the strength reduction factor due to heating (ψ_T), defined earlier in equation (6), was calculated. Figure 19 shows the variation of ψ_T with the exposure temperature T normalized by T_g for the dataset of 55 FRP-strengthened specimens. From Figure 19, a proposed predictive model for estimation of ψ_T can be given by

$$\psi_T = \begin{cases} 1.0 \text{ for } T \le 0.5T_g \\ \dfrac{8}{7} - \dfrac{2}{7}\left(\dfrac{T}{T_g}\right) \text{ for } 0.5T_g \le T \le 4T_g \end{cases} \tag{7}$$

In the above equation, an upper bound of $T = 4T_g$ was imposed because for a temperature exceeding this limit, the confined compressive strength may be less than the unconfined compressive strength at room temperature as seen in Figure 19 for two specimens, for which ψ_T became negative. The proposed predictive equation was then converted to a design model such that there are no non-conservative data points as seen in Figure 19. The proposed design equation for calculation of ψ_T is thus given by

$$\psi_T = \begin{cases} 1.0 \text{ for } T \le 0.5T_g \\ \dfrac{4}{3} - \dfrac{2}{3}\left(\dfrac{T}{T_g}\right) \text{ for } 0.5T_g \le T \le 2T_g \\ 0.0 \text{ for } 2T_g \le T \le T_{\lim} \end{cases} \tag{8}$$

where $T_{\lim}$ is an upper bound for T proposed in this study for limit of FRP effectiveness, and is given by

$$T_{\lim} = \text{minimum of} \begin{cases} 4T_g \\ 300\ ^{\circ}C \\ T_d \end{cases} \tag{9}$$

Table 7. Details and dimensions of specimens tested by other researchers.

	Dimensions				Strengthening system											
Specimen ID	D (mm)	H (mm)	$f'_{co,R}$ (MPa)	$f'_{co,T}$ (MPa)	Type	n	n_s	w_s (mm)	t_f (mm)	E_f (GPa)	f_{fu} (MPa)	T_g (°C)	Exposure temp. (°C)	Exposure time (h)	$f'_{cc,T}$ (MPa)	Notes
Tests by Al-Salloum et al.[19]																
CFRP-R	100	200	38.8	38.8	CFRP	1	1	200	1	77.28	846	88	27	–	95.4	Room temp.
CFRP-100-1h	100	200	38.8	38.2	CFRP	1	1	200	1	77.28	846	88	100	1	94.7	
CFRP-100-2h	100	200	38.8	38.1	CFRP	1	1	200	1	77.28	846	88	100	2	94.5	
CFRP-100-3h	100	200	38.8	37	CFRP	1	1	200	1	77.28	846	88	100	3	90.5	
CFRP-200-1h	100	200	38.8	36.1	CFRP	1	1	200	1	77.28	846	88	200	1	77.5	
CFRP-200-2h	100	200	38.8	35.3	CFRP	1	1	200	1	77.28	846	88	200	2	74.5	
CFRP-200-3h	100	200	38.8	34.2	CFRP	1	1	200	1	77.28	846	88	200	3	69.4	
GFRP-R	100	200	38.8	38.8	GFRP	1	1	200	1.3	27.6	552	88	27	–	69.6	Room temp.
GFRP-100-1h	100	200	38.8	38.2	GFRP	1	1	200	1.3	27.6	552	88	100	1	66.7	
GFRP-100-2h	100	200	38.8	38.1	GFRP	1	1	200	1.3	27.6	552	88	100	2	65.2	
GFRP-100-3h	100	200	38.8	37	GFRP	1	1	200	1.3	27.6	552	88	100	3	61.7	
GFRP-200-1h	100	200	38.8	36.1	GFRP	1	1	200	1.3	27.6	552	88	200	1	61.1	
GFRP-200-2h	100	200	38.8	35.3	GFRP	1	1	200	1.3	27.6	552	88	200	2	58.8	
GFRP-200-3h	100	200	38.8	34.2	GFRP	1	1	200	1.3	27.6	552	88	200	3	58.0	
Tests by Cleary et al.[17]																
GFRP-R	200	400	39.9	39.9	GFRP	2	1	400	1.3	26.1	575	121	21	–	104.3	Room temp.
GFRP-120	200	400	39.9	NA	GFRP	2	1	400	1.3	26.1	575	121	120	1.5	102.3	
GFRP-135	200	400	39.9	NA	GFRP	2	1	400	1.3	26.1	575	121	135	1.5	100.2	
GFRP-150	200	400	39.9	NA	GFRP	2	1	400	1.3	26.1	575	121	150	1.5	91.1	
GFRP-180	200	400	39.9	NA	GFRP	2	1	400	1.3	26.1	575	121	180	1.5	85.2	
Tests by Ponmalar[36]																
GF_1-R	150	300	18.9	18.9	GFRP	1	1	300	0.13	72	2270	132	27	–	31.5	Room temp.
GF_2-R	150	300	18.9	18.9	GFRP	2	1	300	0.13	72	2270	132	27	–	43.3	Room temp.
GF_3-R	150	300	18.9	18.9	GFRP	3	1	300	0.13	72	2270	132	27	–	47.7	Room temp.
GF_1-200	150	300	18.9	15.5	GFRP	1	1	300	0.13	72	2270	132	200	3	27.2	

(continued)

Table 7. Continued

Specimen ID	Dimensions				Strengthening system								Exposure temp. (°C)	Exposure time (h)		Notes
	D (mm)	H (mm)	$f'_{co,R}$ (MPa)	$f'_{co,T}$ (MPa)	Type	n	n_s	w_s (mm)	t_f (mm)	E_f (GPa)	f_{fu} (MPa)	T_g (°C)			$f'_{cc,T}$ (MPa)	
GF_2-200	150	300	18.9	15.5	GFRP	2	1	300	0.13	72	2270	132	200	3	40.0	
GF_3-200	150	300	18.9	15.5	GFRP	3	1	300	0.13	72	2270	132	200	3	45.0	
Tests by El-Din and Mohamed[37]																
CFRP-3S-R	100	200	18.8	18.8	CFRP	1	3	40	0.17	230	3900	68	21	NA	31.0	Room temp.
CFRP-F-R	100	200	18.8	18.8	CFRP	1	1	200	0.17	230	3900	68	21	NA	53.3	Room temp.
CFRP-3S-100	100	200	18.8	18.1	CFRP	1	3	40	0.17	230	3900	68	100	NA	29.9	
CFRP-F-100	100	200	18.8	18.1	CFRP	1	1	200	0.17	230	3900	68	100	NA	50.9	
CFRP-3S-150	100	200	18.8	16.6	CFRP	1	3	40	0.17	230	3900	68	150	NA	26.7	
CFRP-F-150	100	200	18.8	16.6	CFRP	1	1	200	0.17	230	3900	68	150	NA	48.4	
CFRP-3S-200	100	200	18.8	11.1	CFRP	1	3	40	0.17	230	3900	68	200	NA	24.7	
CFRP-F-200	100	200	18.8	11.1	CFRP	1	1	200	0.17	230	3900	68	200	NA	38.8	
Tests by El-Gamal et al.[38]																
CFRP-R	100	200	21.44	21.44	CFRP	1	1	200	0.13	225	3500	71	27	–	54.9	Room temp.
CFRP-100-3h	100	200	21.44	18.64	CFRP	1	1	200	0.13	225	3500	71	100	3	54.7	
CFRP-200-3h	100	200	21.44	18.62	CFRP	1	1	200	0.13	225	3500	71	200	3	52.6	
CFRP-300-2h	100	200	21.44	18.9	CFRP	1	1	200	0.13	225	3500	71	300	2	53.5	
CFRP-300-3h	100	200	21.44	18.57	CFRP	1	1	200	0.13	225	3500	71	300	2	41	
GFRP-R	100	200	21.44	21.44	GFRP	1	1	200	0.35	70	1000	71	27	–	33.77	Room temp.
GFRP-100-1h	100	200	21.44	21.72	GFRP	1	1	200	0.35	70	1000	71	100	1	30.61	
GFRP-100-2h	100	200	21.44	20.41	GFRP	1	1	200	0.35	70	1000	71	100	2	30.01	
GFRP-100-3h	100	200	21.44	18.64	GFRP	1	1	200	0.35	70	1000	71	100	3	27.82	
GFRP-200-1h	100	200	21.44	23.03	GFRP	1	1	200	0.35	70	1000	71	200	1	27.14	
GFRP-200-2h	100	200	21.44	19.44	GFRP	1	1	200	0.35	70	1000	71	200	2	27.14	
GFRP-200-3h	100	200	21.44	18.62	GFRP	1	1	200	0.35	70	1000	71	200	3	23.07	
GFRP-300-1h	100	200	21.44	20.19	GFRP	1	1	200	0.35	70	1000	71	300	1	22.48	
GFRP-300-2h	100	200	21.44	18.9	GFRP	1	1	200	0.35	70	1000	71	300	2	22.48	
GFRP-300-3h	100	200	21.44	18.57	GFRP	1	1	200	0.35	70	1000	71	300	3	20.96	

D: specimen diameter; H: specimen height; $f'_{co,R}$: compressive strength of unconfined concrete at room temperature; $f'_{co,T}$: compressive strength of unconfined concrete at elevated temperature; n: no. of plies of FRP reinforcement; n_s: no. of FRP strips; w_s: width of FRP strip; t_f: thickness of one ply of FRP reinforcement; E_f: tensile modulus of elasticity of FRP material; f_{fu}: tensile strength of FRP material; T_g: glass transition temperature of epoxy adhesive; $f'_{cc,T}$: compressive strength of FRP-confined concrete at elevated temperature.

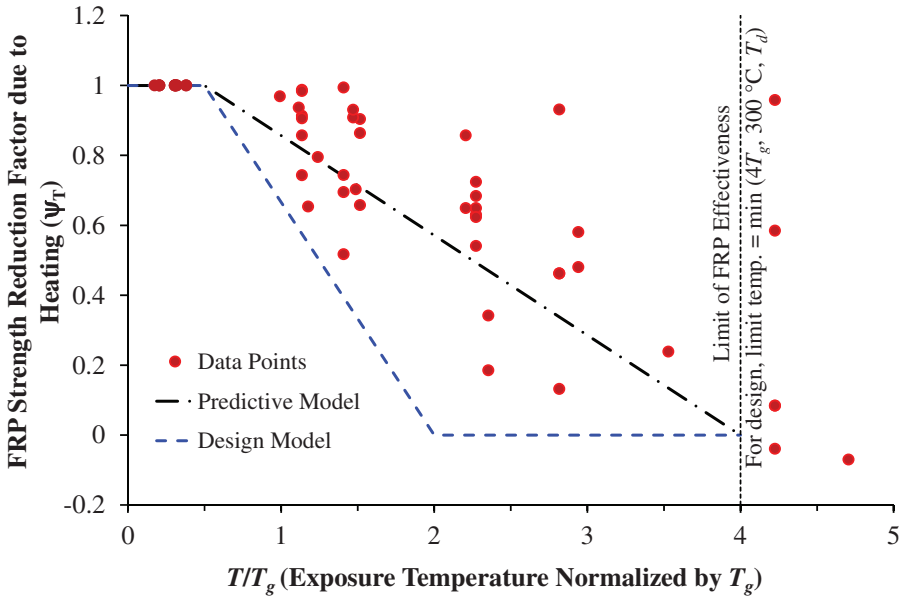

Figure 19. Variation of FRP strength reduction factor due to elevated temperature (ψ_T) with exposure temperature.

where T_d = thermal decomposition temperature of the epoxy matrix. It should be noted that in the proposed design model in equation (8), the FRP wrapping is considered effective in increasing the axial strength of columns after their exposure to elevated temperatures below $2T_g$. For elevated temperatures between $2T_g$ and T_{lim}, the FRP strengthening may be only successful at restoring the original capacity of the unstrengthened column. Yet, for temperatures in excess of T_{lim}, the axial strength of the FRP-upgraded column may be less than that of the unstrengthened column at room temperature and the FRP jacket is deemed ineffective in increasing or even restoring the original axial capacity of the unstrengthened column. In such a case, the axial capacity of the column may be computed using models that estimate the strength of unconfined concrete after high temperature exposure.[39,40]

Excluding both the 12 specimens at room temperature and the 6 specimens with temperatures exceeding the upper bound T_{lim} given in equation (9), the experimental database was reduced to 37 specimens. For these 37 specimens, both the original and modified equation of the ACI 440.2R-08 guidelines were used to predict the confined concrete compressive strength. The predicted results were plotted versus the experimental data as depicted from Figure 20. It is obvious from Figure 20(a) that the original ACI model of equation (2) is non-conservative for a significant portion of the data (about 48.6%) and therefore it cannot be used in estimating the confined concrete strength for FRP-strengthened columns after elevated temperature

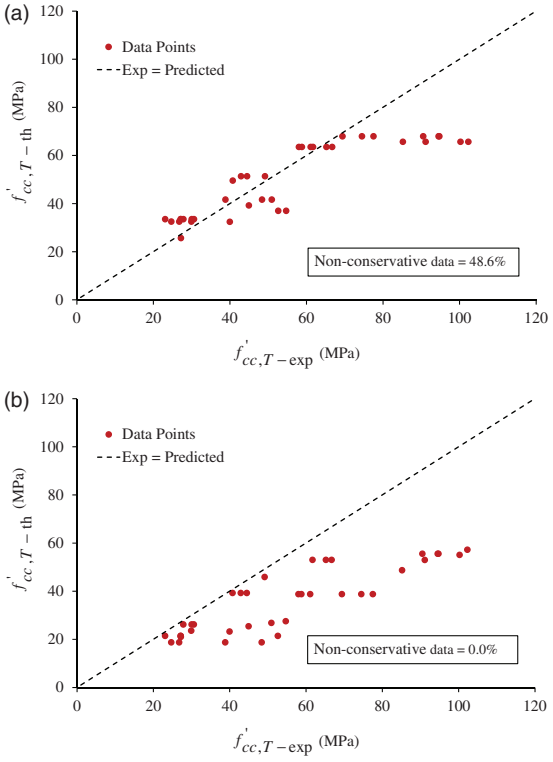

Figure 20. Comparison of confined concrete compressive strength at elevated temperature predicted by original and modified models of ACI 440.2R-08 with experiment. (a) Original ACI model (equation (2)) and (b) modified ACI model (equation (3)).

exposure. However, as depicted from Figure 20(b), equation (3) (modified version of the original ACI model) is conservative for all data points and can be used successfully in estimating the compressive strength of FRP-strengthened columns after high temperature exposure.

Conclusions

The major conclusions derived from this research can be summarized as follows:

1. Exposure to elevated temperature adversely impacts the residual strength, stiffness, and axial/lateral stress–strain response of unstrengthened RC circular columns tested under uniaxial compression after cooling down to ambient. The reductions in compressive strength observed in the current study are consistent with data available in the literature.
2. For both room and elevated temperature exposures, all FRP-strengthened specimens tested in this study failed by rupture of the FRP sheets.
3. For both unstrengthened and FRP-strengthened columns, the reduction in residual stiffness due to heating was greater than the reduction in their residual axial load capacity. Since the load shared by columns of multistory buildings relies mainly on their relative stiffness, a detailed evaluation of residual stiffness has to be conducted for all RC columns after exposure to fire or elevated temperature environments including the columns that are not in direct contact with the heating or fire source.
4. Externally bonded FRP composites could be used effectively in enhancing the axial load capacity of RC columns provided that the temperature at the FRP level does not exceed the decomposition limit of the epoxy resin. This conclusion is consistent with previous research available in the literature on fire-exposed FRP-strengthened RC columns.
5. A comparison between the strengthening systems has revealed that the reduction in both strength and stiffness was higher in CFRP-strengthened columns compared with the GFRP-strengthened columns. This was due to the nonappearance of voids and the impenetrable structure of the glass fibers used which aided in the protection of the epoxy resin from the detrimental effects of the high temperatures.
6. The insulation material used in this study was found to be effective in preventing heat induced damage to CFRP-strengthened columns up to temperatures of 800°C for 3 h duration. This is evident from the fact that the compressive strength enhancement ratio did not reduce below the service load level of the CFRP-strengthened column specimens thereby demonstrating the insulation effectiveness in preventing the column collapse at this level of temperature exposure.
7. The rate of temperature increase plays an important role in the performance of concrete under elevated temperature regimes. For the same target temperature, as the rate of temperature rise increases the loss in concrete strength becomes more pronounced.
8. The ACI 440.2R-08 model used for assessing compressive strength of FRP-confined concrete was evaluated for case of RC circular columns after their exposure to elevated temperatures using the results of 55 specimens (7 columns tested in this study and 48 columns tested by other researchers). This model was found non-conservative for 48.6% of the data and was therefore revised by the inclusion of an FRP strength reduction factor due to heating (ψ_T). The modified ACI model can be employed to estimate the concrete strength of FRP-wrapped columns after exposure to elevated temperatures ranging from ambient to $T_{\lim}$, where $T_{\lim}$ is an upper bound for T proposed in this study for limit of FRP effectiveness, and is taken as the minimum of: $4T_g$, thermal decomposition temperature of the epoxy matrix (T_d) and 300°C.

Declaration of Conflicting Interests

The author(s) declared no potential conflicts of interest with respect to the research, authorship, and/or publication of this article.

Funding

The author(s) disclosed receipt of the following financial support for the research, authorship, and/or publication of this article: The project was supported by Deanship of Scientific Research Chairs at King Saud University, Saudi Arabia, for MMB Chair of Research and Studies in Strengthening and Rehabilitation of Structures at Civil Engineering Department.

References

1. Moshiri N, Hosseini A and Mostofinejad D. Strengthening of RC columns by longitudinal CFRP sheets: Effect of strengthening technique. *Constr Build Mater* 2015; 79: 318–325.
2. Al-Karaghool HO. *Strength and ductility of axially loaded RC short columns confined with CFRP and GFRP wraps*. MS Thesis, The American University of Sharjah, United Arab Emirates, 2013.
3. Chikh N, Gahmous M and Benzaid R. Structural performance of high strength concrete columns confined with CFRP sheets. In: *Proceedings of the world congress on engineering (WCE)*, Vol. III, July 4–6, 2012, London, UK.

4. Quiertant M and Clement J-L. Behavior of RC columns strengthened with different CFRP systems under eccentric loading. *Constr Build Mater* 2011; 25: 452–460.
5. Gajdošová K and Bilčík J. Slender reinforced concrete columns strengthened with fibre reinforced polymers. *Slovak J Civil Eng* 2011; XIX: 27–31.
6. Olivová K and Bilčík J. Strengthening of concrete columns with CFRP. *Slovak J Civil Eng* 2009; 1: 1–9.
7. Benzaid R, Chikh N and Mesbah H. Study of the compressive behavior of short concrete columns confined by fiber reinforced composite. *Arab J Sci Eng* 2009; 34: 15–26.
8. Al-Salloum YA. Influence of edge sharpness on the strength of square concrete columns confined with composite laminates. *Compos Part B-Eng* 2007; 38: 640–650.
9. Elsanadedy HM, Almusallam TH, Abbas H, et al. Effect of blast loading on CFRP-Retrofitted RC columns – a numerical study. *Lat Am J Solids Struct* 2011; 8: 55–81.
10. Elsanadedy HM, Al-Salloum YA, Abbas H, et al. Prediction of strength parameters of FRP confined concrete. *Compos Part B-Eng* 2012; 43: 228–239.
11. Elsanadedy HM, Al-Salloum YA, Alsayed SH, et al. Experimental and numerical investigation of size effects in FRP wrapped concrete columns. *Constr Build Mater* 2012; 29: 56–72.
12. Siddiqui NA, Alsayed SH, Al-Salloum YA, et al. Experimental investigation of slender circular RC columns strengthened with FRP composites. *Constr Build Mater* 2014; 69: 323–334.
13. Haroun MA, Mosallam AS, Feng MQ, et al. Experimental investigation of seismic repair and retrofit of bridge columns by composite jackets. *J Reinf Plast Comp* 2003; 22: 1243–1268.
14. Haroun MA and Elsanadedy HM. Numerical models for composite-jacketed reinforced concrete bridge columns. *J Reinf Plast Comp* 2003; 22: 1203–1219.
15. Apicella F and Imbrogno M. Fire performance of CFRP-composites used for repairing and strengthening concrete. In: *Proceedings of the 5th ASCE materials engineering congress*, Cincinnati, Ohio, 1999, pp.260–266.
16. Bisby LA. *Fire behaviour of FRP reinforced or confined concrete*. PhD Thesis, Kingston, Canada: Department of Civil Engineering, Queen's University, 2003.
17. Cleary DB, Cassino CD and Tortorice R. Effect of elevated temperatures on a fiber composite to strengthen concrete columns. *J Reinf Plast Comp* 2003; 22: 881–895.
18. Saafi M and Romine P. Effect of fire on concrete cylinders confined with GFRP. In: Benmokrane B and EI-Salakawy E (eds) *Durability of fibre reinforced polymer (FRP) composites for construction*, CDCC 02, Quebec, Canada: Université de Sherbrooke, 2002.
19. Al-Salloum YA, Elsanadedy HM and Abadel AA. Behavior of FRP-confined concrete after high temperature exposure. *Constr Build Mater* 2011; 25: 838–850.
20. Khalifa A, El-Kurdi A, Eldarwish A, et al. Effect of elevated temperature on structural performance of R.C. columns confined By CFRP. In: *The 2nd official regional conference of international institute for FRP in construction for Asia-pacific region* (APFIS), Seoul, Korea, 9–11 December 2009, pp.463–473.
21. El-Karmoty HZ. Thermal protection of reinforced concrete columns strengthened by GFRP laminates (experimental and theoretical study). *HBRC J* 2012; 8: 115–122.
22. Chowdhury EU, Bisby LA, Green MF, et al. Investigation of insulated FRP-wrapped reinforced concrete columns in fire. *Fire Safety J* 2007; 42: 452–460.
23. Cree D, Chowdhury E, Green M, et al. Performance in fire of FRP-strengthened and insulated reinforced concrete columns. *Fire Safety J* 2012; 54: 86–95.
24. ULC. CAN/ULC-S101-M04. *Standard methods of fire endurance tests of building construction and materials*. Scarborough, ON: Underwriters' Laboratories of Canada, 2004.
25. ASTM. ASTM E119-01. *Standard methods of fire test of building construction and materials*. West Conshohocken, PA: American Society for Testing and Materials, 2001.
26. American Concrete Institute (ACI). *Building code requirements for structural concrete and commentary*. *ACI 318-14*, Detroit, MI: American Concrete Institute, 2014.
27. ASTM. *Standard test method for compressive strength of cylindrical concrete specimens*. ASTM C39/C39M, West Conshohocken, PA: American Society for Testing and Materials, 2010.
28. ASTM. *Standard test methods for tension testing of metallic materials*. ASTM E8/E8M, West Conshohocken, PA: American Society for Testing and Materials, 2009.
29. Khalifa T. *The effects of elevated temperatures on fibre reinforced polymers for strengthening concrete structures*. MS Thesis, Queen's University, Kingston, Ontario, Canada, 2011.
30. ASTM. ASTM D3039/D3039M – 08. *Standard test method for tensile properties of polymer matrix composite materials*. West Conshohocken, PA: American Society for Testing and Materials, 2008.
31. ISO. *Fire-resistance tests – elements of building construction – part 1: General requirements*, ISO 834-1:1999. Geneva, Switzerland: International Organization for Standardization, 1999.
32. Freskakis GN, Burrow RC and Debbas EB. *Strength properties of concrete at elevated temperature*. *Civil engineering nuclear power, ASCE national convention*. Boston, USA: American Society of Civil Engineering, 1979.
33. American Concrete Institute (ACI). *Guide for the design and construction of externally bonded FRP systems for strengthening concrete structures*. *ACI 440.2R-08*. Detroit, MI: American Concrete Institute, 2008.
34. Foster SK and Bisby LA. High temperature residual properties of externally bonded. FRP systems. In: *Proceedings of the 7th international symposium on fiber reinforced polymer reinforcement for reinforced concrete structures (FRPRCS-7)*, SP-230-70, 2005, pp.1235–1252. Farmington Hills, MI, USA: American Concrete Institute (ACI).
35. Kodur V, Bisby LA and Green MF. FRP retrofitted concrete under fire conditions. *J Concrete Int* 2006; 28: 37–44.

36. Ponmalar V. Strength comparison of fiber reinforced polymer (FRP) wrapped concrete exposed to high temperature. *Int J Appl Sci Eng Res* 2012; 1: 146–151.
37. El-Din HS and Mohamed HA. Effect of temperature on strength of concrete strengthening with CFRP. *Int J Eng Sci Innovative Technol (IJESIT)* 2012; 2: 285–294.
38. El-Gamal S, Al-Jabri K, Al-Mahri A, et al. Effects of elevated temperatures on the compressive strength capacity of concrete cylinders confined with FRP sheets: An experimental investigation. *Int J Polym Sci* 2015; 2015: Article 549187.
39. Fédération Internationale du Béton (fib). *Model code 2010 – Final draft*, Vol. 1, Bulletin 65, and Vol. 2, Bulletin 66. Lausanne, Switzerland, 2012.
40. Youssef MA and Moftah M. General stress–strain relationship for concrete at elevated temperature. *Eng Struct* 2007; 29: 2618–2634.